ICAS 2021 SHANG HAI
International Council of the Aeronautical Sciences
32nd Congress of the International Council of the Aeronautical Sciences
September 6-10, 2021 Pudong Shangri-La, Shanghai, China

FURTHER DEVELOPMENT OF COMPUTATIONAL STUDY ON COANDĂ BLANKET CURVATURE EFFECTS ON HALF-SPHERICAL COANDĂ DEVICE

Harijono Djojodihardjo [1] Mohamad Arif Andira[1] Ratih Julistina[2], Mohammad Agoes Moeljadi[2]

[1] *The Institute for the Advancement of Aerospace Science and Technology, Jakarta, Jakarta, Indonesia 1*
Corresponding author; *harijono.djojodihardjo@gmail.com;*
[2] *CCIT Group Indonesia, Depok, West Java, 16425, Indonesia 2*
[3] *Faculty of Mechanical and Aerospace Engineering, Institut Teknologi Bandung, Bandung, Indonesia 3*

Abstract

Further development to gain better understanding on the principle of Coandă MAV lift generation, and following the mathematical model for a spherical Coandă MAV developed and analyzed earlier from first physical principles is elaborated. Surface curvature is an important parameter that greatly affects the lift generation performance of an aerodynamic body which has relative motion with respect to the fluid, as demonstrated by airfoils and aircraft wings. Therefore, the influence of curvature of the Coandă blanket on the lift generation performance of a Coandă MAV will be the focus of the present investigation. CFD simulation for a Coandă MAV generic model with several surface curvatures are elaborated. Parametric studies on the effect of various relevant variables are also presented.

Three types of curvature were analyzed utilizing a Coandă MAV with selected baseline dimensional parameters for proof of concept. To this end, a six-degree Bernstein polynomial representing an elliptical curve and a logarithmic spiral curve with two different characteristic coefficients are employed. These three configurations were tested on 5 different aspect ratios from 0.7 to 1.0. To gain basic understanding of the principles of Coandă MAV lift generation, including the relationship between relevant parameters, the mathematical model for a semi-spherical Coandă MAV based on first principles as employed in earlier works was utilized. Noting that the influence of viscosity is the essential factor that will influence the performance of the Coandă MAV, CFD simulations were carried out and elaborated to verify as well as to obtain more realistic lift generation performance compared to those theoretically predicted using first principles for potential flow. The CFD software used for this purpose is made available by CCIT Group Indonesia and utilizes Menter SST k-ω turbulence model. Results obtained are considered encouraging, and wil be utilized as some of the bases for further evaluation of the Coandă MAV lift generation and realated works.

Keywords: Aerodynamics, Applied Aerodynamics,Coandă, Computational Fluid Dynamics, Micro Air Vehicle

1. Introduction

Since its founding, Coandă effect and Coandă jet have been found and utilized for flow control in many applications in engineering and health science, among others, such as in aircraft and vehicle technology and wind-turbines [1]. In a seminal report on the effects of streamline curvature on turbulent flow, Bradshaw [2] categorized the tendency of a fluid jet placed near a surface to attach itself to the surface, and the attached jet growing more rapidly. He subdivided the Coandă effect into three distinct phenomena, which are illustrated in Figure 1. The effect whereby a jet attached to a convex surface grows more rapidly than the wall jet on a plane surface, according to [2, 3], should be more appropriately referred to as 'Coandă effect'.

Based on such considerations and preliminary results reported in [4, 5, 6, 7, 8, 9, 10], further work for CFD simulations and associated parametric study will be carried out, guided by a hypothetic flow situation schematically modeled in Figure 2. This Figure has been synthesized using information obtained in these and other references, and depicts estimated flow structure in and around the Coandă blanket for the Coandă device.

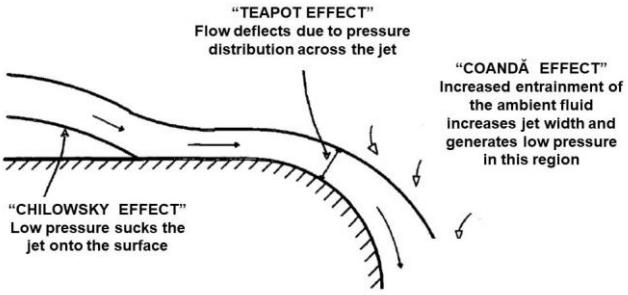

Figure 1 Coandă Flow Characteristic

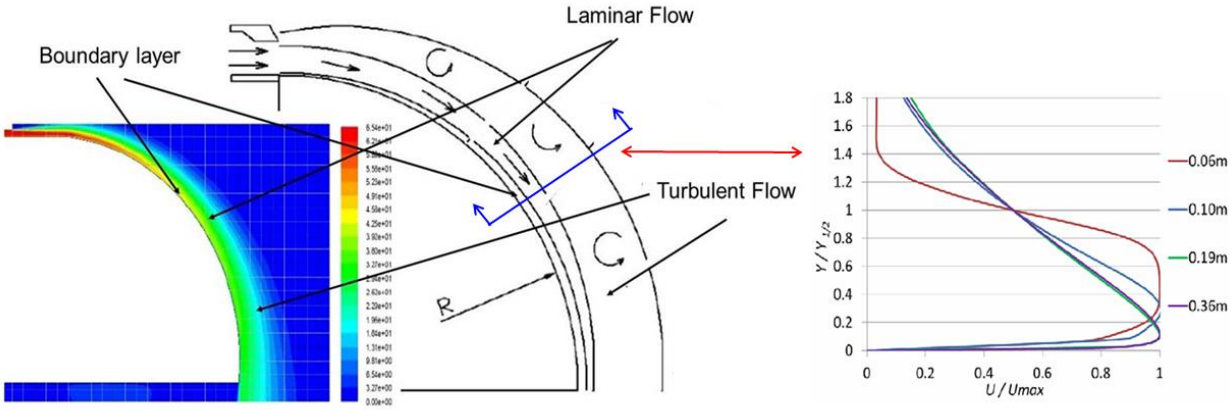

Figure 2. COANDĂ Jet over curved surface and preliminary flow structure estimate

For a Coandă MAV, lift is produced in two ways. First, due to the change of direction of the airflow downwards, or momentum exchange, between the outflow and inflow, and second, due to pressure differential between the lower and upper side of the MAV body or Coandă device, among others due to the entrainment of air from the surrounding air which causes a region of low pressure above the body. Hence, the main objective of the present work is to obtain relevant information on the Curvature effects on a half-spherical Coandă device performance, qualitatively and to some extent, quantitatively.

2. CFD Simulation Studies on Coandă effect on Spherical Coandă Device.[1]

Earlier works by the authors on Coandă Effects has the objectives to understand how the jet flow around a half sphere ejected at various distances between the jet flow outlet from the stagnation point of the half sphere may generate lift (or thrust), and the associated viscous fluid flow phenomena.

These series of CFD Simulation Studies on Coandă effect on Spherical Coandă Device will be followed by further curvature effects on the Coandă Device performance. The diameter of the input jet outlet has been set as the reference length. This configuration is utilized for the CFD simulation in this section, and is exhibited in Figure 3 as the first baseline configuration.

The main objective of the CFD Simulation Studies on Coandă effect on Spherical Coandă Device in this section is to study the flow pattern, to obtain more realistic information which will modify the first principle analysis on the potential fow case carried out earlier. The distance h between the incoming jet outlet is varied from one to five times of the incoming jet outlet diameter. Without loss of generalities, the incoming jet velocity is set to be 1.025 m/s in the CFD simulation.

[1] CFD All Simulations presented in this section is carried out by Dr. Mochammad Agoes Moeljadi at the Institute of Technology Bandung using Fluent.

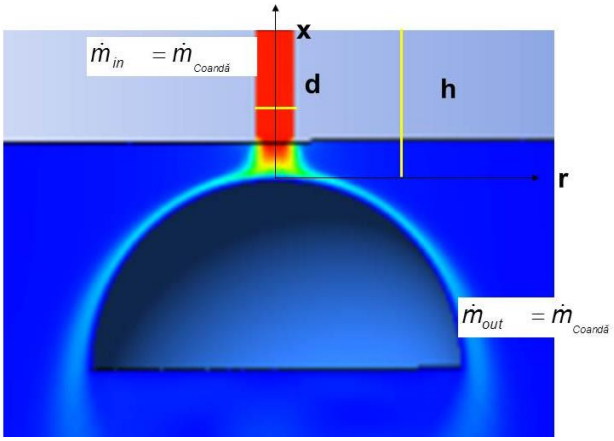

Figure 3 A semi-spherical Coandă MAV configuration for CFD Flow Pattern Analysis

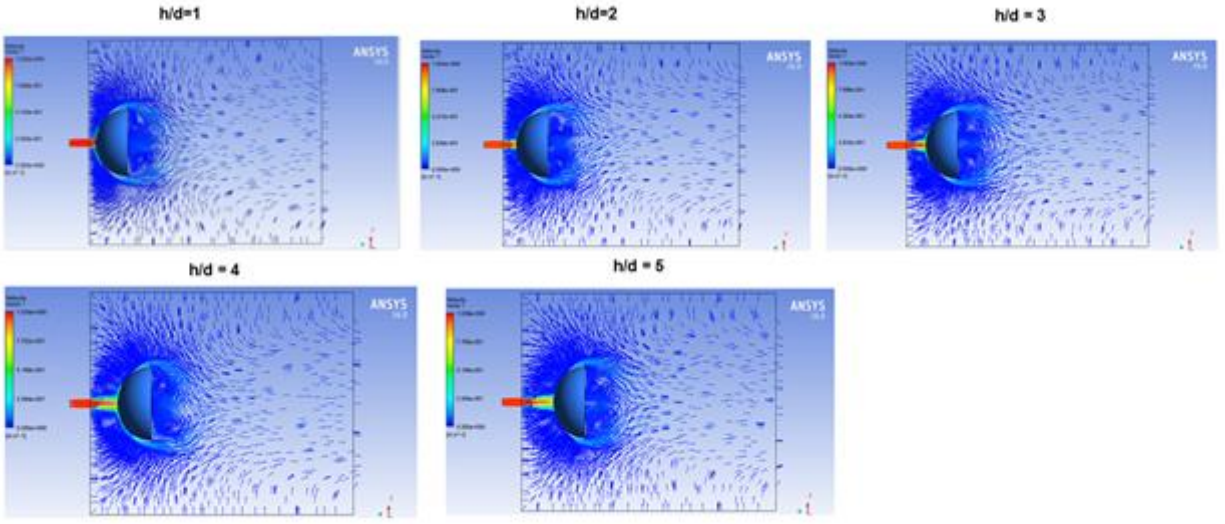

Figure 4 CFD Simulation Studies for the influence of h/d on the Velocity Vector. h/d is varied from 1 to 5

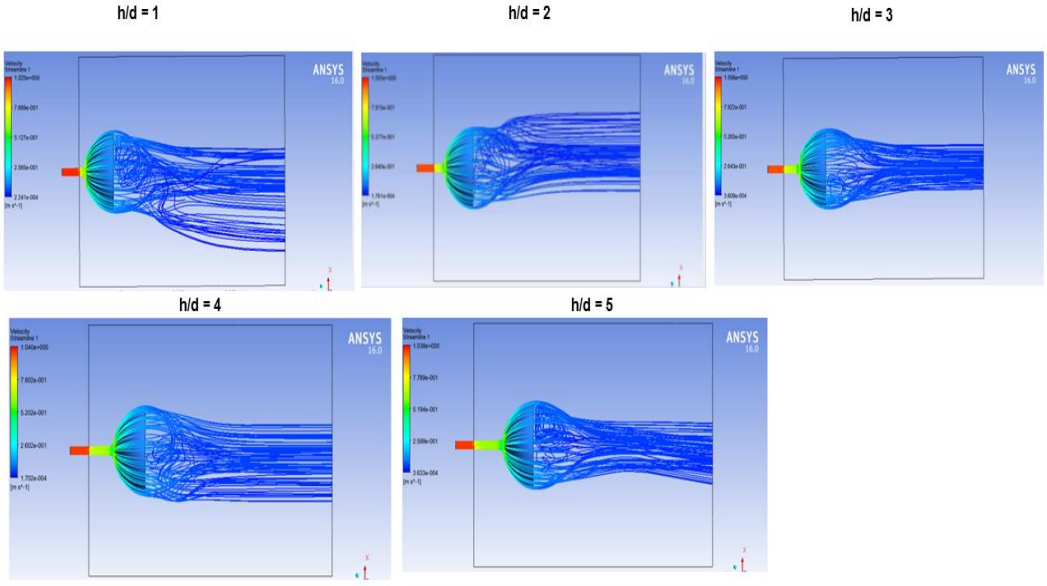

Figure 5 CFD Simulation Studies for the influence of h/d on the Streamline. h/d is varied from 1 to 5

Figures 4, 5 and 6 illustrated CFD simulation studies for the baseline Coandă MAV configuration depicted in Figure 3, by varying the distance h of the incoming jet orifice with diameter d to the top or stagnation point of the Coandă MAV upper surface. In the CFD simulation, h/d is varied from 1 to 5 with an increment of one. Three types of simulation images are presented; figure 4 exhibits the velocity vector, Figure 5 the streamlines, and Figure 6 the velocity ontour.

It can be observed, that after exiting from the orifice at the center of the Coandă device, and assuming initial uniform flow profile across the width of the jet, the jet follows closely the surface of the Coandă device downstream. Eventually, at or near the end of the Coandă device, after passing the trailing edge of the half sphere, the flow separates forming wake flow. The flow structure in the wake is random and generating two circulating flows (for two dimensional images; actually, in three-dimensional axi-symmetrical case, the flow is similar to an irregular ringlike pattern) as depicted by the velocity vector arrows in Figure 4. The jet flow with higher velocity compared to the surrounding ambient fluid and viscous effects occurring in the vicinity of the wall may indicate that thrust or lift is generated. Arriving downstream as a wake, the Coandă jet then deflected downward as shown in Figures 5 and 6.

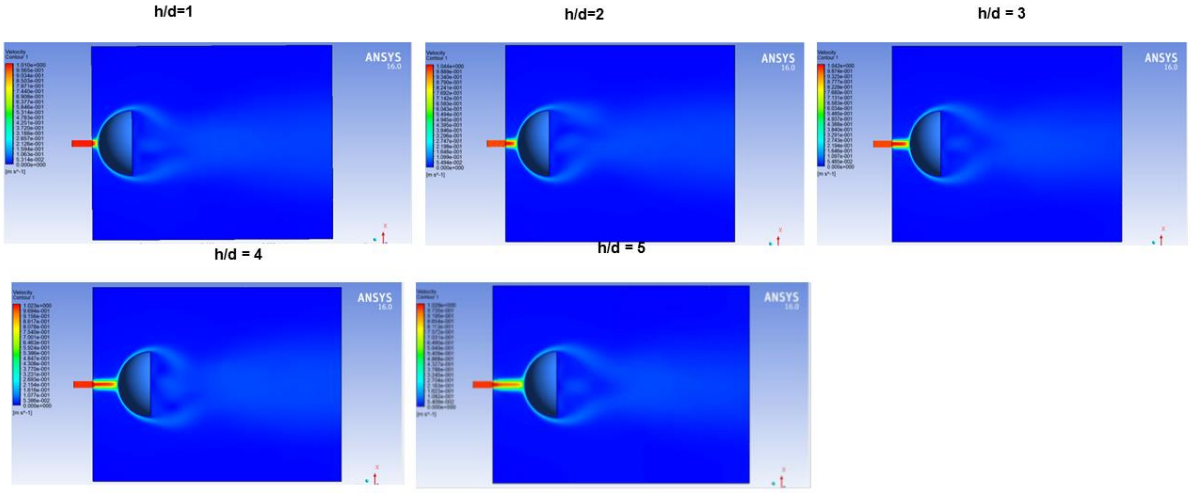

Figure 6 CFD Simulation Studies for the influence of h/d on the Velocity Contour. h/d is varied from 1 to 5

The state of affairs of the Coandă effects on the Coada device geometry utilized as elaborated will be the subject of analysis, in addition to the second part of the investigation which is elaborated subsequently.

3. Coandă MAV Geometric Configuration

In this section, the geometry of the Coandă device will be investigated. Two options will be considered in creating the geometries of the curvature of the Coandă MAV Geometric Configuration.

For comparative and bench marking purposes, six-degree Bernstein polynomial as employed by Mirkov and Rasuo [4, 11, 12, 13] and logarithmic spiral curve studied previously by Gan et al. [8] will be considered.

It is noted that any two-dimensional curvatures of airfoils, axially symmetric bodies, and other more complex three-dimensional shapes can be represented by means of the class function and shape function within the 'CST' approach (Class/shape transformation method) [14, 15, 16, 17]. The class function determines a general class of geometries, whereas the shape function aims to define particular shapes within the geometrical class.

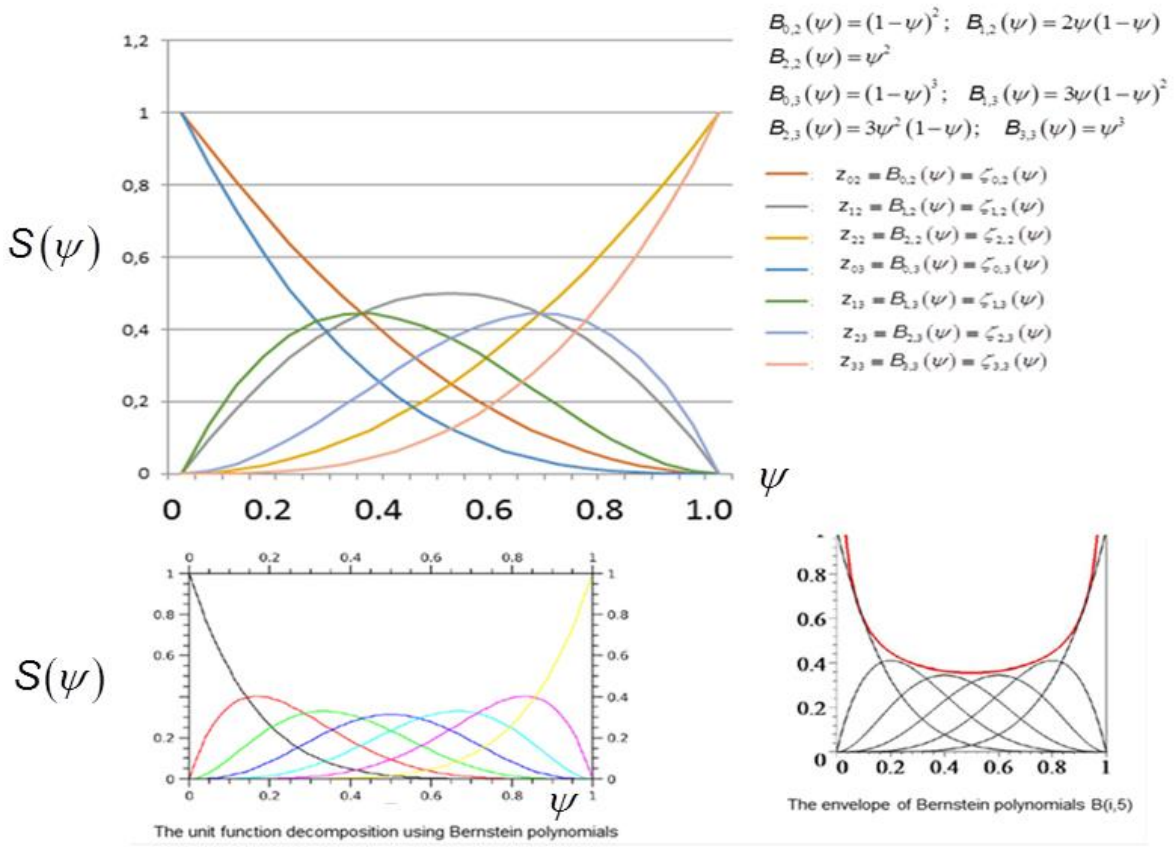

Figure 7 Impressions of Sample Curves of Bernstein Polynomial of Sixth Degree

The main idea behind this method is to decompose the basic shape into scalable elements associated with the discrete components by representing the shape function with a Bernstein polynomial. The Bernstein polynomial of order n can be written as

$$S_{r,n}(\psi)=K_{r,n}\psi^2(1-\psi)^{n-r} \tag{1}$$

where

$$K_{r,n}\equiv\binom{n}{r}=\frac{n!}{r!(n-r)} \tag{2}$$

where the factors $K_{r,n}$ are binomial coefficients. Figure 7 shows an example of unit function decomposition using Bernstein polynomials of sixth degree in an overall impression of sample curves of Bernstein Polynomial of Sixth Degree.

The geometry of the cross section of the Coandă MAV considered is identical to an elliptic arc; therefore the class function used in this study will be the function representing an elliptic arc,

$$\zeta(\psi)=A\psi^{0.5}(1-\psi)^{0.5} \tag{3}$$

Then the chosen polynomial for the surface curvature of the geometry is defined by the following expressions. The upper contour is defined by

$$C_{upper}(\psi)=\zeta(\psi)S(\psi) \tag{4}$$

where

$$\zeta(\psi) = 0.7\psi^{0.5}(1-\psi)^{0.5} \tag{5}$$

and

$$S(\psi) = 1 \tag{6}$$

Here, the aspect ratio, i.e., the ratio between the Coandă MAV radius and its height is determined with the value A of 0.7. Finally, the value of the parameter ψ resides in the interval $\psi \in [0,1]$. The only difference with the work of Mirkov and Rasuo [4] is that the current lower surface is a flat (straight) line.

In comparison to the Bernstein Polynomial curvature, the second method taken from the work of Gan et.al. [8] uses a combination of a flat plate of length l and a logarithmic spiral curve as given by the following polar equation

$$r(\theta) = ae^{b\theta} \tag{7}$$

where a denotes the aspect ratio (similar to A in the Bernstein polynomial), b guides the tightness and direction of the spiral, and θ is calculated from 0^o to 90^o. The baseline configuration of a Coandă MAV utilizing this curvature equation is depicted in Figure 8 below.

Next, the conversion from polar coordinate to Cartesian coordinate can be readily performed by using the following equations

$$x(r,\theta) = r\sin\theta \tag{8}$$

$$y(r,\theta) = r\cos\theta \tag{9}$$

The present study varies the value of b in Equ. (7) between -.03 and 0. The negative value of b causes the logarithmic curve to be more outward but gives steeper transition from the flat plane to the curved surface. The three different curvatures employed to investigate the influence of Coandă blanket curvature on the lift generation performance of a Coandă MAV based on the sixth-degree Bernstein polynomial and the logarithmic spiral curve equation are exhibited in Figure 7.

4 Mathematical Model for a Semi-Spherical Coandă MAV

The mathematical model of a semi-spherical Coandă MAV developed here is based on previous works of Ahmad et al. [17] and Djojodihardjo [5, 6, 7, 18, 19]. It utilizes first physical principles and conservation equations to determine the amount of lift generated by the Coandă MAV. Performance measure variable, denoted as $\mathbf{PM_p}$, is introduced to assess the performance of the generated lift due to the pressure difference with respect to the rate of momentum input. The relationships between the relevant parameters of the mathematical model of the Coandă MAV to lift generation are summarized subsequently.

Coandă MAV uses a propeller or a centrifugal fan that is mounted on top of the body at the center axis. For conceptual development purposes, the small dimension of the rotor can be accepted as a valid assumption. The air being drawn by the rotor will flow in radial direction throughout the Coandă blanket surface and is presumed to be utilized entirely for lift generation. In deriving the mathematical model, the control volume of the Coandă MAV as physically modeled in Figure 8 is drawn covering the simplified generic model as illustrated by the red dashed line in Figure 9.

As carried out in previous studies, the analysis of the Coandă effect in producing lift on a 3-dimensional Coandă MAV will be based on first principles: the momentum conservation principle as also represented by the Euler equation, if the viscosity effects are ignored. . The flow is also assumed to be steady and incompressible.

Considering these prevailing assumptions, the continuity equation applied to the control volume

enclosing the Coandă blanket can be written as

$$\dot{m}_{in} = \dot{m}_{out} \tag{10}$$

$$2\pi \rho R_i h_i V_{j-in} = 2\pi \rho R_o h_o V_{j-out} \tag{11}$$

$$V_{j-out} = \frac{R_i h_i}{R_o h_o} V_{j-in} = \frac{\dot{m}_{in}}{2\pi \rho R_o h_o} \tag{12}$$

where V_j represents the jet inlet velocity both into and out of the control volume. R is the MAV body radius, h is the j

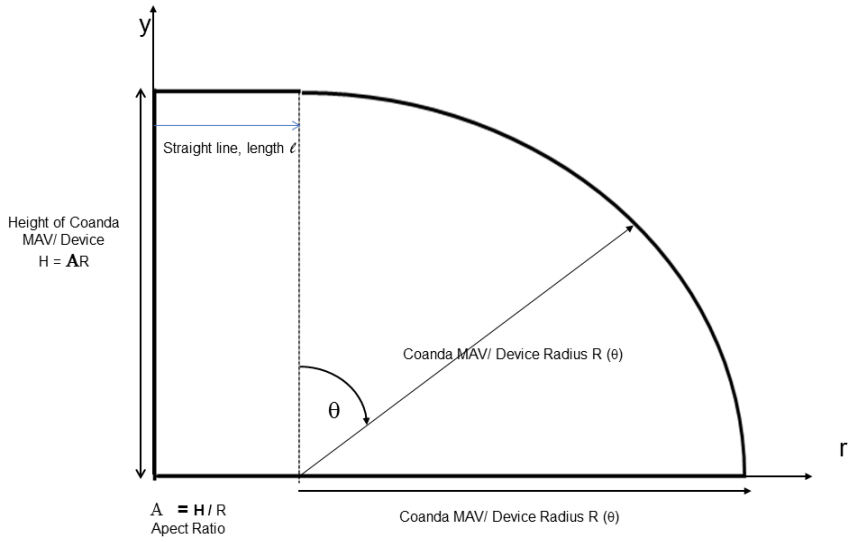

Figure 8 The Coandă MAV baseline configuration using the logarithmic spiral curved equation.

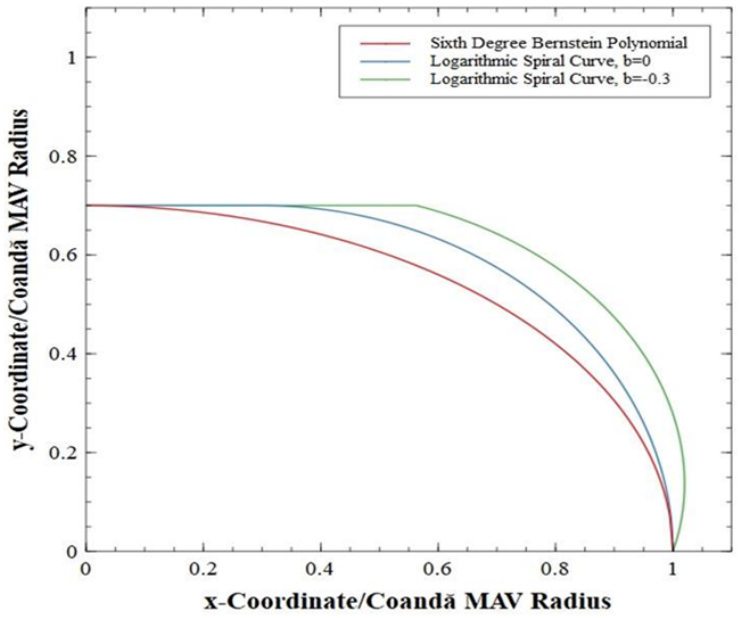

. Figure 9 Three different Coandă MAV curvatures used in the present study

The subscripts i (or in) and o (or out) denote the inner and outer portion of the Coandă blanket respectively. As depicted in Figure 11, the Coandă blanket is subject to the ambient static pressure ,

which then becomes the prevailing static pressure on it. The lift force can be determined by applying the momentum equation in y (vertical) direction, which can be further classified into two components; vertical component of momentum balance and pressure difference on the body.

First principles analysis of the Coandă effects on lift produced a 3-D Coandă MAV

$$\begin{pmatrix} Total\ Lift\ Force\ due\ to \\ Coanda\ Effects \end{pmatrix} = \begin{pmatrix} Vertical\ Component\ of \\ momentum\ flux\ balance \\ due\ to\ Coanda\ Blanket \end{pmatrix} + \begin{pmatrix} \mathrm{Pr}\,essure\ adifference\ on\ the \\ Coanda\ Device\ Blanket \end{pmatrix} \quad (13)$$

The lift force due to the vertical momentum flux balance throughout the control volume CV is given by

$$\begin{pmatrix} Force\ in\ the \\ y-direction \end{pmatrix} = \begin{pmatrix} Rate\ of\ momentum \\ influx\ into\ CV\ in \\ the\ y-direction \end{pmatrix} + \begin{pmatrix} Rate\ of\ momentum \\ flux\ out\ of\ CV\ in \\ the\ y-direction \end{pmatrix} \quad (14)$$

In the radial direction, the momentum in does not contribute to the lift, the momentum equation in the y-direction for the CV depicted in Figures 10 and 11 is

$$\begin{aligned} F_{Coanda\ Jet\ Blanket} &= \dot{m}_{out} V_{j-out} \\ &= \dot{m}_{in} V_{j-out} = 2\pi\rho R_i h_i V_{j-in} V_{j-out} \end{aligned} \quad (15)$$

Figure 10 illustrates also a different Coandă MAV/ Device Baseline Configuration for CFD simulation studies. Here, the diameter of the cylindrical flow inlet, which is equivalent to the diameter of the propeller utilized to produce the radial jet flow, is welldefined and is utilized in the analysis using first principles

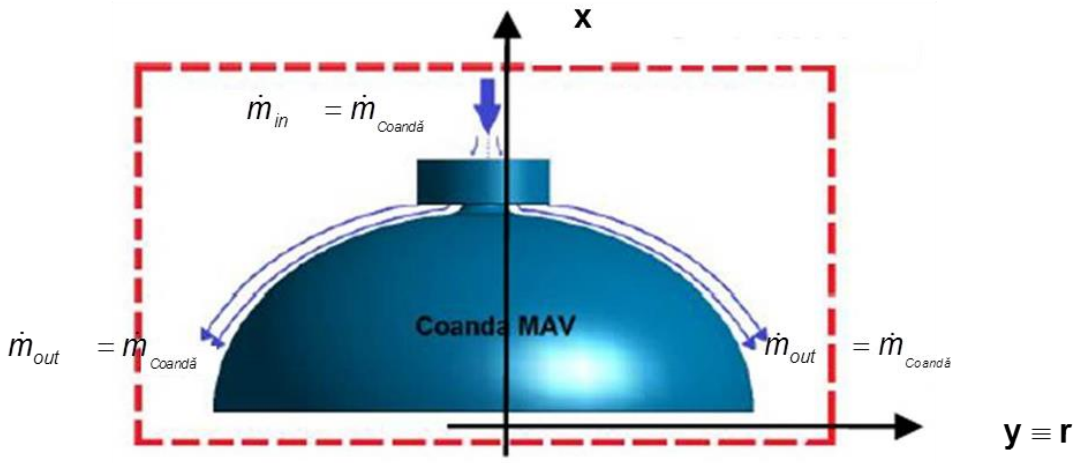

Figure 10. A semi-spherical based Coandă MAV as the other baseline configuration, as it may apply, for control volume for generic analysis

The contribution of lift from the pressure difference between the upper (curved MAV body covered by Coandă Blanket) and the lower part of the MAV body is rigorously elaborated in Djojodihardjo [5]. Figure 11 provides an illustration regarding θ_i and θ_o which are the turning angle at which the jet flow is injected to and is separated from the Coandă surface, respectively. The outflow jet velocity is assumed to be uniform in a such a way that the contribution of the pressure difference across the Coandă blanket surface designed to generate lift for the significant value of θ_i is expressed by

$$F_{\substack{induced\\pressure\\difference}} = F_{\substack{lower\\surface}} - F_{\substack{upper\\surface}} = \dot{m}\int_{R_{j-in}}^{R_{j-out}} \frac{V_{j-out}}{R_j} dR_j$$
$$= \dot{m}V_{j-in}\left(\ln R_{j-out} - \ln R_{j-in}\right) \quad (16)$$

Hence, the total amount of lift generated by the Coandă MAV due to the Coandă jet vertical momentum and the Coandă blanket pressure difference is

$$L_{CoandaMAV} = 2\pi\rho R_i h_i V_{j-in} V_{j-out} + \dot{m}V_{j-in}\left(\ln R_{j-out} - \ln R_{j-in}\right) \quad (17)$$

$$L_{CoandaMAV} = \dot{m}V_{j-out} + \dot{m}V_{j-in}\left(\ln R_{j-out} - \ln R_{j-in}\right) \quad (18)$$

Therefore, the Coandă MAV has additional lift given in equation (18), due to the presence of the Coandă blanket, in comparison to a simple micro air vehicle powered by actuator disk only. Also, solving equation (14) will directly give the lift force value if the value of Vj-out is known. However, the case is that $V_{j\text{-}out}$ appears as an unknown variable that must be determined before calculating the Coandă MAV lift. Consequently, a more exact approach requires additional information, i.e. the energy conservation equation, which is then employed as the fourth equation. Applying the energy conservation on the same control volume, assuming uniform properties across the sectional areas at the input and output of the Coandă jet blanket and ignoring the entrainment energy exchange between the ambient air and the Coandă jet blanket, the energy equation can be written as

$$\left(\frac{p}{\rho}\right)_{in} + \frac{1}{2}V_{j-in}{}^2 = \left(\frac{p}{\rho}\right)_{out} + \frac{1}{2}V_{j-out}{}^2 \quad (19)$$

which is essentially the Bernoulli equation along any streamline between the inlet and the outlet sections. The contribution of the entrainment energy exchange along the Coandă jet blanket can later be incorporated, such as by adopting certain assumptions as a heuristic approach.

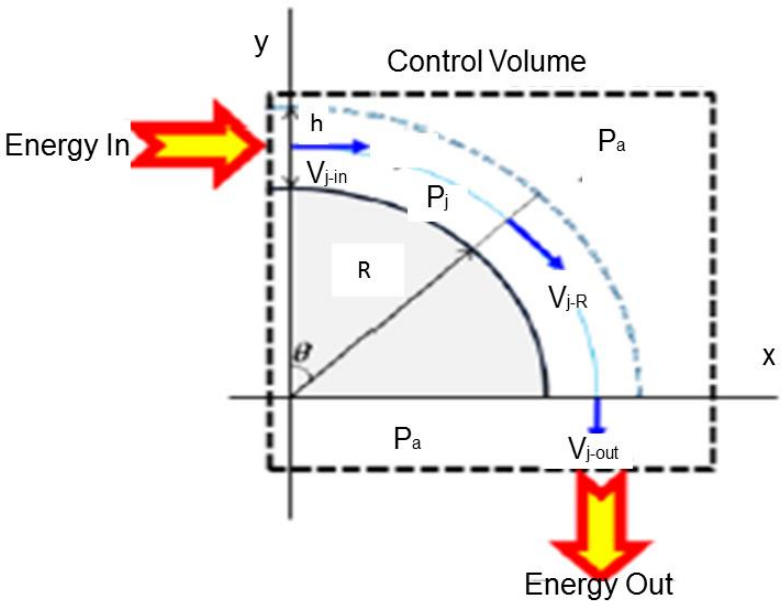

Figure 11 Schematic of the energy conservation of a Coandă jet blanket

Using Figure 10 and Figure 11 as a basis and noting that from the outset, the flow is considered to be incompressible, since

$p_{in} = p_{out} = p_{\text{ambient-air}}$,

and

$$\dot{m}_{in} = \dot{m}_{out} \ ,$$

equation (15) can be reduced to

$$\frac{1}{2} V_{j-in}{}^2 = \frac{1}{2} V_{j-out}{}^2 \tag{20}$$

or

$$V_{j-in} = V_{j-out} \tag{21}$$

This equation should significantly simplify the solution given by equation (14). Substituting equation (17) to equation (14) yields

$$L_{CoandaMAV} = \dot{m} V_{j-in} \left(1 + \ln \frac{R_{j-out}}{R_{j-in}} \right) \tag{22}$$

The coefficient of lift is obtained by simply dividing the lift force by the dynamic pressure times wetted area of Coandă blanket given by

$$C_{L-CoandaMAV} = \frac{\dot{m} V_{j-in} \left(1 + \ln \frac{R_{j-out}}{R_{j-in}} \right)}{\frac{1}{2} \rho V_{j-in}{}^2 S_{Conda\,Blanket}} \tag{23}$$

The solution of equation (18), (19) and (23) will be compared to the CFD simulations, which incorporate the viscous effect through the use of Reynolds-Averaged Navier-Stokes (RANS) equation, to assess the validity of first principles assumptions as well as to assess the influence of viscous effects. It is now convenient to calculate (or estimate) the performance of the generated lift of the Coandă MAV during hover and lift-off through the introduction of a non-dimensional quantities of performance measure. For this purpose, the Coandă jet momentum coefficient defined by Poisson-Quinton [21, 22, 23] as

$$C_{\mu} = \frac{\dot{m} V_{j-in}}{\frac{1}{2} \rho V_{j-in}{}^2 S_{Conda\,Blanket}} = \frac{2\pi \rho R_i h_i V_{j-in}{}^2}{\frac{1}{2} \rho V_{j-in}{}^2 S_{Conda\,Blanket}} \tag{24}$$

After some algebra, it can readily be shown that

$$C_{\mu-rotor} = \frac{2\pi \rho R_{j-in} h_{j-in} V_{j-in}{}^2}{\frac{1}{2} \pi R_{R(rotor)}{}^2 \rho U_{R(rotor)}{}^2} = 4 \left(\frac{h_{j-in}}{R_{j-in}} \right) \left(\frac{V_{j-in}}{U_{R(rotor)}} \right)^2 \tag{25}$$

Performance Measure PM can be defined as the Total Lift/ Rate of Momentum Input, and is an indicator of the effectiveness of the Coandă jet device (MAV) to produce lift from rotor-like momentum rate input from the ambient air. In these earlier references, a heuristic model for the total lift was assumed. Physically, the performance measure PM delineates the amplification of the input force through fluid mechanics mechanism which is an analogy the notion of lever in engineering equipment. From the analytical point of view, the performance measure value will always be greater than one since the outer radius of the Coandă MAV blanket is larger than the inner radius. This also needs to be verified with CFD simulations which accounts for viscous force in the momentum equation resulting in a variation of velocity in the normal direction to the Coandă wall, in contrast with the derivation of the mathematical model where the velocity is assumed to be uniform along a certain streamline.

$$PM_{Coanda} = \frac{Lift}{(Rate\,of\,Momentum\,Input)_{CoandaMAV}} = \frac{\dot{m}V_{j-in}\left(1+\ln\frac{R_{j-out}}{R_{j-in}}\right)}{2\pi\rho R_{j-in}h_{j-in}V_{j-in}^{\ 2}} = \left(1+\ln\frac{R_{j-out}}{R_{j-in}}\right) \quad (26)$$

The Performance Measure **PM**[2] can alternatively be written in terms of momentum coefficient as

$$PM_{Coanda} = \frac{Lift}{(Rate\,of\,Momentum\,Input)_{CoandaMAV}} = \frac{\dot{m}V_{j-in}\left(1+\ln\frac{R_{j-out}}{R_{j-in}}\right)}{2\pi\rho R_{j-in}h_{j-in}V_{j-in}^{\ 2}} \approx 4\frac{h_{j-in}}{R_{j-in}}\frac{V_{j-in}^{\ 2}}{U_{R(rotor)}^{\ 2}}\frac{\left(1+\ln\frac{R_{j-out}}{R_{j-in}}\right)}{C_{\mu-Rotor}} \quad (27)$$

which is valid for a Coandă MAV configuration with actuator (rotor) fully dedicated to produce Coandă Jet Blanket.

5 CFD Simulations of Coandă MAV for Coandă Surface Curvature Effect on Lift

CFD simulations were performed using CFDSOF® software developed by CCIT Group Indonesia based on OpenFOAM® with several enhancements and integrated interactive graphical user interface. Moreover, a specific mesh generator was developed and derived from the main software for the purpose of this research.

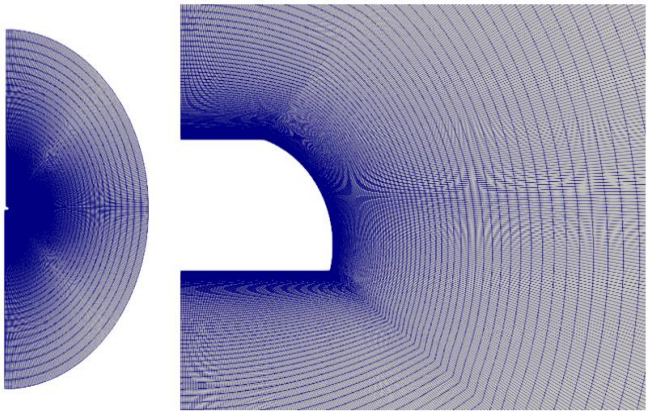

a b

Figure 12 (a) 2D O-grid axi-symmetric domain; (b) clustered mesh near the Coandă MAV surface[3]

The motivation was to efficiently tackle the parameterized geometrical problem of a Coandă MAV. By utilizing this program, one only needs to input geometrical parameters, such as Coandă

[2] The Performance Measure PM has been utilized in all previous author and coworkers publication. In the present work, an alternative term Figure of Merit **FM** is introduced and can be used alternatively

[3] All CFD Simulations presented in this section is carried out by Mohamad Arif Andira and Ratih Julistina using CFD software developed at CCIT Group Indonesia.

MAV radius, height, jet slot thickness, inner diameter, or even curvature type and the program will automatically generate O-type multi block structured grid with the ability to control the mesh distribution and spacing across the domain.

The 2D-axisymmetric domain is used to reduce computational cost and preserve mesh quality. Furthermore, the layer cells were carefully added near the Coandă MAV wall, including the calculation of value to determine the first cell height required to accurately capture near-wall behavior for the particular turbulence model. To compute the flow field in an efficient manner, the mesh is refined near the walls and get coarser towards the far-field. Before performing further numerical studies, grid independence test was conducted for testing three mesh configurations with number of cells of 54560, 75040, and 116160 respectively against the performance measure based on pressure difference (PMp). The second mesh was chosen to be used for the rest of CFD simulations considering the difference from the highest number of cells was only below 4% with lower computational cost and time.

The flow is assumed to be steady, incompressible, viscous, and turbulent. Hence, the appropriate mathematical model for this study is the Reynolds-Averaged Navier-Stokes (RANS) equations with Menter's Shear-Stress Transport turbulence model. These governing equations are discretized using cell-centered second-order accurate finite volume method. The pressure-velocity coupling in the case of incompressible flow is solved iteratively using SIMPLE algorithm [16]. Since in the incompressible flow, the important variable is the pressure difference and not the absolute value of the pressure itself, thus the far-field boundary is set to have 0 Pa static pressure. The Coandă jet enters the domain through the Coandă inlet with the size of h as depicted in Figure 11 (and simulated in Figure 12) with specified velocity value.

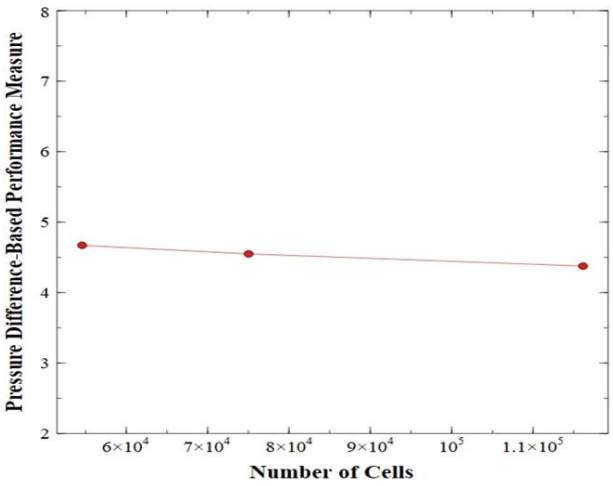

Figure 13 Grid independence test result

6 Results and Discussion

The influence of Coandă blanket curvature on Coandă MAV lift generation performance will be discussed in this section by means of computational fluid dynamics simulation study. The analysis begins with observing the following graphic.

Figure 14 depicts the pressure-based Performance Measure (**PM_p, FM_p**) with respect to the ratio between Coandă MAV Height (h) and Coandă MAV Radius (R), or aspect ratio.

In general, all types of curve exhibit similar trend where for each aspect ratio, the sixth-degree Bernstein polynomial (red curve) has the lowest value of PMp, followed by the logarithmic spiral curve for characteristic coefficient of 0 (blue curve) and -0.3 (green curve) respectively.

The exception occurs for the aspect ratio of 1 where the red curve and blue curve almost coincide, meaning they only have a very small difference. However, this is not the case for the green curve since it has a much greater value than others. This finding can be explained by looking at the Figure 15representing the three curvatures at aspect ratio of 1.

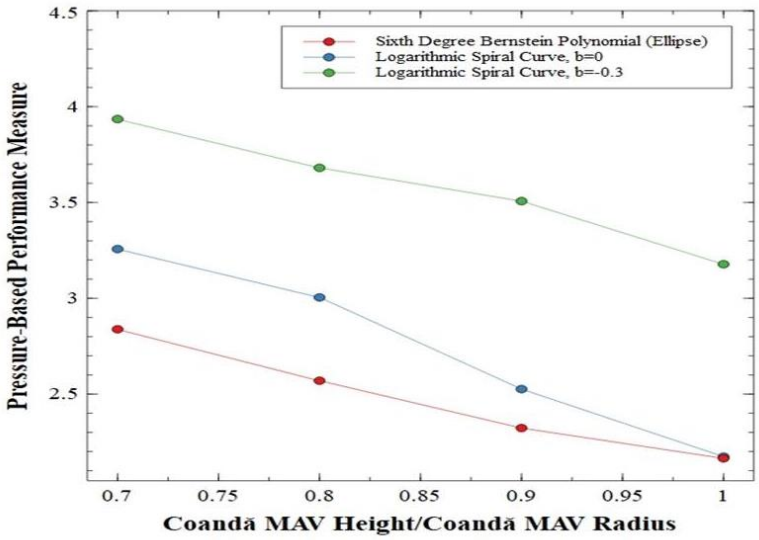

Figure 14 Pressure-based Performance Measure CFD result

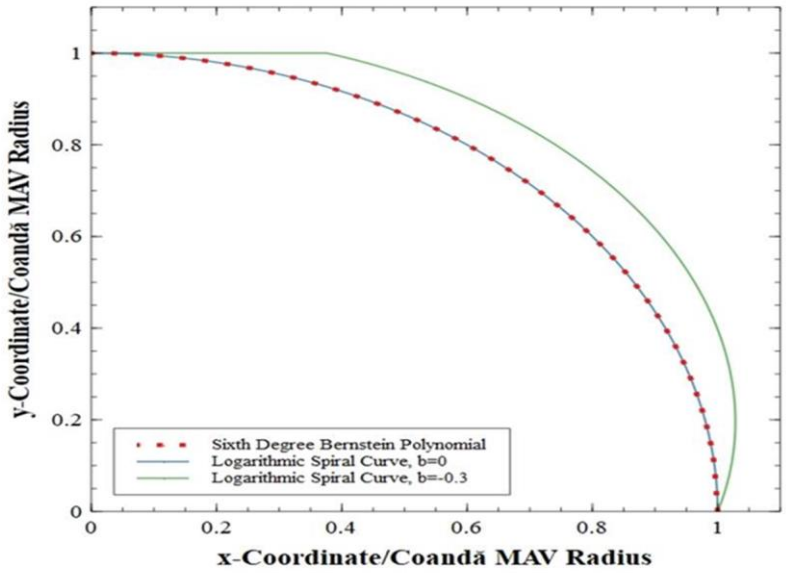

Figure 15 Coandă MAV blanket curvature at h/R = 1

Based on Figure 9 and Figure 15, choosing b equals to zero gives a smooth curvature with some portion of flat line, which value will get smaller as aspect ratio increases. Therefore, when the aspect ratio is 1, the logarithmic curve with zero b coefficient will mimic the ellipse curvature. This geometric behavior also can explain why there is a steep change on blue curvature from aspect ratio 0.8 to 0.9.

One important point from this observation is that the curvature consists of a flat line will produce higher aerodynamic lift, and thus higher lift generation performance as has been proven by the logarithmic spiral curvatures. To obtain more insight about this phenomenon, pressure coefficient distribution along the Coandă blanket is visualized through a number of graphics as follows.

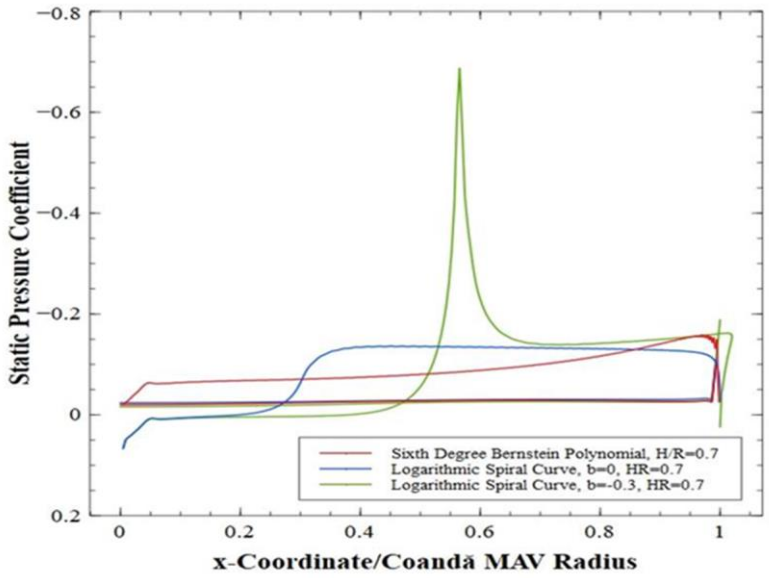

Figure 16 Cp distribution along Coandă MAV blanket at h/R = 0.7

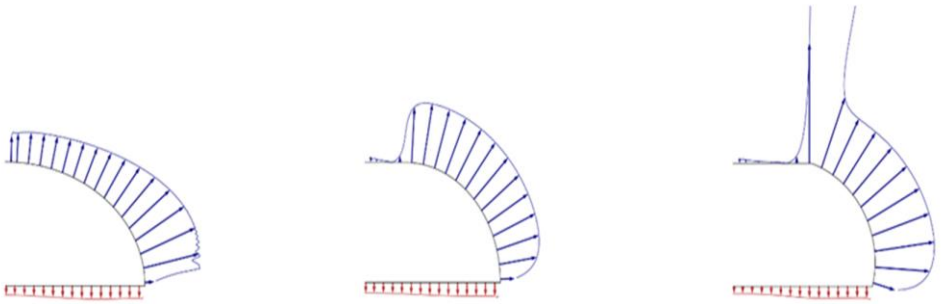

Figure 17 Cp distribution along Coandă MAV blanket at h/R = 0.7. (a) sixth-degree Bernstein polynomial (ellipse), (b) logarithmic spiral curve with b=0, (c) logarithmic spiral curve with b=-0.3

From the sequence of pressure distribution illustrations above, it can be observed that the flat surface has a very low-pressure zone and more uniform pressure distribution across the curved blanket which are favorable for enhancing aerodynamic lift generation performance. Furthermore, the magnitude of static pressure coefficient distribution is also greater for the logarithmic configurations, so that the resulting vacuum pressure in y-direction will be higher which indicates the device will gain better aerodynamic lift. In contrast, the magnitude of static pressure coefficient distribution on the ellipse curvature depicts lower value in the y-direction and increases on the side of the blanket in which the direction will not have much contribution to the overall aerodynamic lift. Hence, this type of curve will have lower lift generation performance.

Figure 18 and Figure 19 provide further information that supports the discussion of the results by providing the flow field contour in terms of velocity magnitude and static pressure. The notable feature from the velocity contour is the flow deflection by the Coandă is different for the three configurations. The ellipse curve tends to bend the air in a straight manner in negative y-direction while the logarithmic curve steers the air flow toward the symmetry axis.

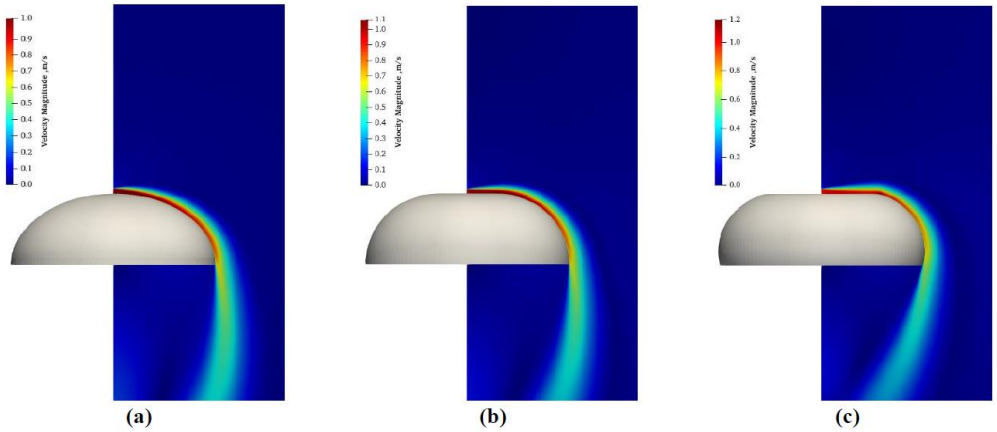

Figure 18 Velocity magnitude contour around the Coandă MAV at h/R = 0.7. (a) sixth-degree Bernstein polynomial (ellipse), (b) logarithmic spiral curve with b=0, (c) logarithmic spiral curve with b=-0.3

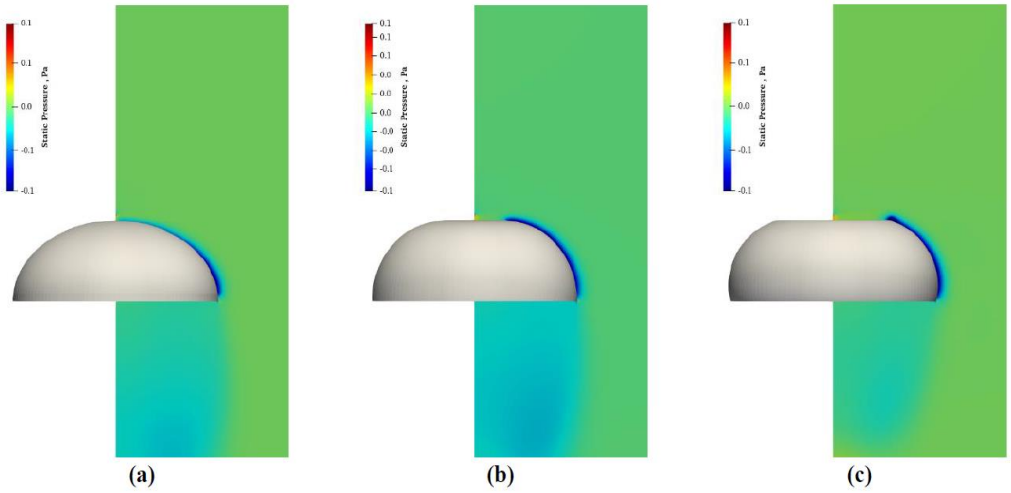

Figure 19 Static pressure contour around the Coandă MAV at h/R = 0.7. (a) sixth-degree Bernstein polynomial (ellipse), (b) logarithmic spiral curve with b=0, (c) logarithmic spiral curve with b=-0.3

7 Conclusion

The work reported in 2018 and the present one lead to the following conclusion:
The associated effects of the Coandă effect concluded from these studies are as follows.

- Velocity profile is thinner and the distance of maximum velocity to the surface is nearer on the curved surface compared with that on a flat plane.
- Jet width grows proportionally along the curved surface.
- Surrounding air is entrained into the jet flow, as shown by the increase in mass flow.
- A jet suddenly accelerates at the start of the curve, and the maximum velocity decay along the curved surface is proportional.
- Surface pressure is lower than atmospheric pressure on a surface with a sudden drop at the start of the curve.
- With varying exit jet heights, the development trend of the flow along the Coandă surface is observed to be similar but with different change rates.
- The overall parametric analysis of varying exit jet heights shows that the effective range of d/R is 0.1 to 0.14.
- The parametric study shows that the Coandă effect achieves stable performance after certain geometric variations, which can lead to the conclusion that an optimal design solution for a

Coandă UAV exists.

CFD Simulation Studies for three different configurations based on the flow situation schematically modeled in Figure 2, which depicts estimated flow structure in and around the Coandă blanket for the Coandă device, which has been synthesized using information obtained in the references [1- 9]

lead to the following summary and conclusions

- The first design is based on the sixth-degree Bernstein polynomial, with particularly chosen coefficients can represent an ellipse. The other configurations are employed the logarithmic spiral curvature with some portion of flat surface, with two distinct characteristic coefficients.
- The lift generation performance is significantly affected by the device curvature. In particular, a curvature with flat surface and steeper side results a better performance due to the wider vacuum pressure zone on the top flat surface and more uniform and favorable, higher magnitude pressure coefficient distribution across the blanket.
- The same configuration can produce a greater amount of lift by reducing the aspect ratio, i.e., the ratio between the Coandă height and Coandă radius.

Further work:

- Exploring another class of curvature, studying the effects of lower blanket curvature
- More detailed analysis of the flow field, including the jet width growth and boundary layer separation point.
- Further experimental investigations to develop a flying prototype that is based purely on the Coandă effect.
- The numerical results obtained thus far can be used for further experimental investigations to develop a flying prototype that is based purely on the Coandă effect.

References

[1] Djojodihardjo H and Thangarajah N, “Research, Development and Recent Patents on Aerodynamic Surface Circulation Control - A Critical Review,” Recent Patents on Mechanical Engineering, vol. 7, no. 1, pp. 1–37, 2014, doi: 10.2174/2212797607666140204004542.

[2]. P. Bradshaw, Effects of streamline curvature on turbulent flow, Advisory Group for Aerospace Research and Development, Paris, France (1973). [2]. Gad-el-Hak, M., Flow Control: Passive, Active, and Reactive Flow Management, Cambridge University Press, Cambridge, England, 2007.

[3]. S. Cutbill, A study of the turbulent flow of a high speed Coandă jet, PhD Thesis, U Durham, 1998

[4]. Mirkov, N. and Rasuo, B., Numerical Simulation of Air Jet Attachment to Convex Walls and Application to UAV, in Boundary and Interior Layers, Computational and Asymptotic Methods - BAIL 2014, DOI: 10.1007/978-3-319-25727-3_15

[5]. Djojodihardjo, H., Overview On The Influence Of Coandă Blanket Curvature On Coandă Device Performance, Proceedings, ICAS 2018, Belo Horizonte, Brazil.

[6]. Djojodihardjo, H., Ahmed, R. I., “An Analysis on the Lift Generation for Coandă Micro Air Vehicles,” IEEE International Conference on Aerospace Electronics and Remote Sensing, Yogyakarta, 2014., doi: 10.13140/2.1.2150.4320

[7]. Djojodihardjo, H., Ahmed, R. I., Abu Talib, A. R., Mohd Rafie, A. S., “First Principles Analysis of Coandă Micro Air Vehicle Aerodynamic Forces for Preliminary Sizing,” Aircraft Engineering and Aerospace Technology, Vol. 89, No. 2, 2017, pp. 231-245.

[8] Gan, C., Sahari, K. S., Tan, S., “Numerical investigation on Coandă flow over a logarithmic surface,” Journal of Mechanical Science and Techonology, Vol. 29, No. 7, 2015, pp. 2863-2869.

[9] Radespiel,R., Burnazzi, M., Fundamentals in Coanda Flap Design, Springer-Verlag Berlin Heidelberg 2011.

[10] Pfingsten, K.C and Radespiel,R., Experimental and numerical investigation of circulation

control airfoil, AIAA-2009-533, 2009.

[11]. Bernstein, S., Demonstration du theoreme de Weierstrass fondee sur le calcul des probabilités. Comm. Soc. Math. Kharkov 13(1-2), 1912.

[12]. Rushan Ziatdinov, Bernstein Polynomials and Bernstein-Bezier Curves, 2015,presentation

[13]. http://mathworld.wolfram.com/BernsteinPolynomial.htm

[14] Su,H., Gong, CL, Gu,LX, Three-Dimensional CST Parameterization Method Applied in Aircraft Aeroelastic Analysis, International Journal of Aerospace Engineering 2017(1):1-15

[15]. Kulfan, B. M., "Recent Extensions and Applications of the "CST" Universal Parametric Geometry Representation Method," AIAA Aviation Technology, Integration and Operations Conference, AIAA, Belfast, 2007.doi: 10.2514/6.2007-7709

[16]. Kulfan, B. M., "Universal Parametric Geometry Representation Method," Journal of Aircraft, Vol. 45, No. 1, 2008. doi: 10.2514/1.29958

[17]. Patankar, S. V., "Numerical Fluid Flow and Heat Transfer," Series in computational methods in mechanics and thermal sciences, Taylor & Francis, Oxfordshire, 2018.

[18]. Ahmed, R, I., Djojodihardjo, H., Abu Talib, A. R., Abd Hamid, M. F., "Application of Coandă Jet for Generating Lift for Micro Air Vehicles – Preliminary Design Considerations," Applied Mechanics and Materials, Vol. 629, 2014, pp. 139-144.doi: 10.4028/www.scientific.net /AMM.629.139

[19]. Djojodihardjo, H., Ahmed, R. I., "Analytical, Computational Fluid Dynamics and Flight Dynamics of Coandă MAV," International Conference on Mechanical Engineering and Automation Science, Singapore, 2016, doi: 10.1088/1757-899X/157/1/012002

[20]. Djojodihardjo, H., Overview of Coandă MAV as an Aerial Robotic Platform, Aerial Robots-Aerodynamics, Control and Applications, IntechOpen, London, 2017 doi: 10.5772/intechopen.70157

[21]. Poisson-Quinton, P. (1952) Aircraft wing and flap with boundary layer control. U.S. Patent No. 2,585,676.

[22]. Poisson-Quinton, P., Lepage, L. (1961) Survey of French research on the control of boundary layer and circulation. In: Lachmann, G.V. (ed.) Boundary Layer and Flow Control: Its Principles and Application, vol. 1, pp. 21–73. Pergamon Press, New York

[23]. Y. El Sayed M., N. Beck, P. Kumar, R. Semaan, R. Radespiel, Challenges in the Experimental Quantification of the Momentum Coefficient of Circulation Controlled Wings, In book: New Results in Numerical and Experimental Fluid Mechanics XI, 2018, DOI: 10.1007/978-3-319-64519-3_48

Contact Author Email Address

The contact author email address should appear explicitly in this section to facilitate future contacts. For example, mailto: corresponding@author.com

Copyright Statement